Spectral modeling of channel band shapes in wavelength selective switches

Cibby Pulikkaseril,* Luke A. Stewart, Michaël A. F. Roelens, Glenn W. Baxter, Simon Poole, and Steve Frisken

Finisar Australia, 244 Young st., Waterloo, NSW, 2017, Australia

**cibby.pulikkaseril@finisar.com*

Abstract: A model for characterizing the spectral response of the passband of Wavelength Selective Switches (WSS) is presented. We demonstrate that, in contrast to the commonly used supergaussian model, the presented model offers a more complete match to measured results, as it is based on the physical operation of the optical system. We also demonstrate that this model is better suited for calculation of WSS channel bandwidths, as well as predicting the final bandwidth of cascaded WSS modules. Finally, we show the utility of this model in predicting channel shapes in flexible bandwidth WSS channel plans.

OCIS codes: (060.2330) Fiber optics communications; (060.4265) Networks, wavelength routing; (230.7408) Wavelength filtering devices.

References and links

1. S. Gringeri, B. Basch,V. Shukla, R. Egorov, T. J. Xia, "Flexible architectures for optical transport nodes and networks," IEEE Commun. Mag. **48**, 40–50 (2010).
2. J. D. Downie, and A. B. Ruffin, "Analysis of signal distortion and crosstalk penalties induced by optical filters in optical networks," J. Lightwave Technol. **21**, 1876–1886 (2003).
3. S. Tibuleac, and M. Filer, "Transmission impairments in DWDM networks with reconfigurable optical add-drop multiplexers," J. Lightwave Technol. **28**, 557–598 (2010).
4. T. A. Strasser, and J. L. Wagener, "Wavelength-selective switches for ROADM applications," IEEE J. Sel. Top. Quantum Electron. **16**, 1150–1157 (2010).
5. F. Heismann, "System requirements for WSS filter shape in cascaded ROADM networks," in *Proceedings of the Optical Fiber Communication Conference*, 2010.
6. G. Baxter, S. Frisken, D. Abakoumov, H. Zhou, I. Clarke, A. Bartos, and S. Poole, "Highly programmable wavelength selective switch based on liquid crystal on silicon switching elements," in *Proceedings of the Optical Fiber Communication Conference*, 2006.
7. M. A. F. Roelens, S. Frisken, J. A. Bolger, D. Abakoumov, G. Baxter, S. Poole, B. J. Eggleton, "Dispersion trimming in a reconfigurable wavelength selective switch," J. Lightwave Technol. **26**, 73–78 (2008).
8. J. W. Goodman, "Frequency analysis of optical imaging system," in *Introduction to Fourier Optics*, 3rd ed. (Roberts and Company, 2005).
9. D. M. Marom, D. T. Neilson, D. S. Greywall, C. S. Pai, N. R. Basavanhally, V. A. Aksyuk, D. O. López, F. Pardo, M. E. Simon, Y. Low, P. Kolodner, and C. A. Bolle,"Wavelength-selective 1 x K switches using free-space optics and MEMS micromirrors: theory, design, and implementation," J. Lightwave Technol. **23**, 1620–1630 (2005).
10. R. N. Thurston, J. P. Heritage, A. M. Weiner, and W. J. Tomlinson, "Analysis of picosecond pulse shape synthesis by spectral masking in a grating pulse compressor," *IEEE J. Quantum Electron.*, **QE-22**, 682–696 (1986).
11. P. Wall, P. Colbourne, C. Reimer, and S. McLaughlin, "WSS switching engine technologies," in *Proceedings of the Optical Fiber Communication Conference*, 2007.
12. "ZEMAX Optical Design Program," ZEMAX Development Corporation, USA.
13. D. Marcuse, "Loss analysis of single-mode fiber splices," Bell Syst. Tech. J. **56**, 703–718 (1977).
14. J. F. James, *Spectrograph Design Fundamentals* (Cambridge University Press, 2007).
15. C. Malouin, J. Bennike, and T. J. Schmidt, "Differential phase-shift keying receiver design applied to strong optical filtering," J. Lightwave Technol. **25**, 3536–3542 (2007).

#141439 - $15.00 USD Received 24 Jan 2011; revised 25 Mar 2011; accepted 4 Apr 2011; published 18 Apr 2011

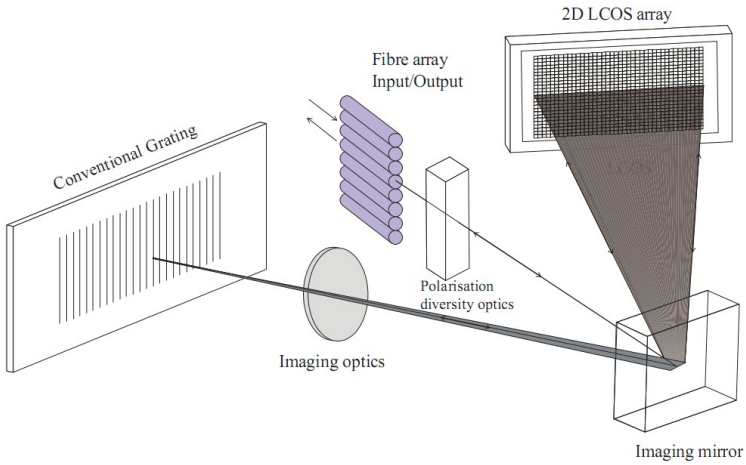

Fig. 1. General schematic of LCoS-based WSS operation as shown in [6].

1. Introduction

Modern optical networks require add/drop nodes to allow efficient routing of signals, necessitating the use of reconfigurable optical add/drop modules (ROADMs) [1]. ROADMs replace passive splitters and multiplexers with Wavelength Selective Switches (WSS), an optical module that allows (de)multiplexing of individual wavelengths to selected common or output ports.

To understand the impact of the WSS channel shape on network performance, it is crucial to have an accurate spectral model of the WSS channel shape, especially as advanced modulation formats are being deployed to increase the spectral efficiency of the network. Early publications have characterized WSS channel shapes with third-order Butterworth filters [2], though this was primarily for thin-film devices. Currently, the literature favours modeling WSS channel shapes with the supergaussian function [3–5], which can be used to roughly match measurements, but is not representative of the underlying physical process, especially when used to predict the performance of a high-bit rate optical link with transmission through multiple ROADM nodes [4, 5].

The WSS structure considered in this letter, shown in Fig. 1, uses a liquid crystal on silicon (LCoS) switching element, as reported in [6]. In this implementation, the input optical signal passes through polarization diversity optics before being incident on a diffraction grating. The diffracted light is then focused onto a 2D array of LCoS pixels, where each pixel is individually addressed and causes a phase retardation from 0 to 2π. In one axis, a phase ramp is created to steer the beam to a desired output fiber [7].

In this letter, we present a method of modeling the channel shape of a WSS. This model is based on the physical operation of the device and it is shown that this model can be generalized to WSS designs that use alternative switching technologies. The model provides some insight into the specification of the WSS, namely that the optical transfer function bandwidth can be a single characterizing parameter of the spectral channel shape. We then demonstrate how this model can be used to predict the bandwidth of cascaded WSS channels, as well as facilitate the prediction of flexible bandwidth channel plans.

#141439 - $15.00 USD Received 24 Jan 2011; revised 25 Mar 2011; accepted 4 Apr 2011; published 18 Apr 2011

2. Theory

2.1. Derivation of bandpass filter power spectrum

We assume that the power spectrum of a single WSS channel, in effect a bandpass filter, is created by an aperture formed at the image plane of spatially diffracted light. For a bandpass filter, this aperture takes the form of a rectangular function, defined in frequency space, given by

$$R(f) = \begin{cases} 1, & -B/2 \leq f \leq B/2 \\ 0, & \text{otherwise,} \end{cases} \tag{1}$$

where B is the width of the rectangular aperture in frequency; for example, a 50 GHz channel would have B = 50 GHz.

The output optical amplitude spectrum of the device is predicted to be the convolution of this aperture function with the optical transfer function (OTF) of the device [8], in this case, assumed to be Gaussian, that is

$$S(f) = \int_{-\infty}^{+\infty} R(f')L(f'-f)df', \tag{2}$$

where $L(f)$ is a normalized Gaussian function given by

$$L(f) = \exp\left[\frac{-f^2}{2\sigma^2}\right], \tag{3}$$

where σ is the standard deviation of the Gaussian OTF and is related to the 3 dB bandwidth by

$$\sigma = \frac{BW_{\text{OTF}}}{2\sqrt{2\ln 2}}. \tag{4}$$

In this analysis, we consider that the OTF bandwidth is a single scalar quantity, constant over the frequency range of the device. The OTF bandwidth of a WSS represents, effectively, how the beam has been focused onto the aperture plane - a smaller OTF bandwidth indicates that the spot size is smaller. We note that a similar parameter is used by Marom et al. for a microelectomechanical system (MEMS)-based WSS, labeled as a "confinement parameter", which has a similar effect on the bandpass filter shape [9].

Completing the integral in Eq. (2) requires the use of the error function; with this, we can express the optical field spectrum of a bandpass filter created by a WSS as

$$S(f) = \frac{1}{2}\sigma\sqrt{2\pi}\left[\text{erf}\left(\frac{B/2 - f}{\sqrt{2}\sigma}\right) - \text{erf}\left(\frac{-B/2 - f}{\sqrt{2}\sigma}\right)\right], \tag{5}$$

where $\text{erf}(x)$ represents the error function. The optical power spectrum of the bandpass filter, to be compared to measurements from an optical spectrum analyzer, is found by squaring Eq. (5) and converting to logarithmic units. We also note that $S(f)$ is the amplitude spectrum of the device, and, as such, is valid for complex values, allowing for prediction of the phase behaviour of WSS channels.

The bandshape predicted by Eq. (5) can also be generated by manipulating Eq. (6) in Marom et al. for the same parameters [9], while a similar expression was shown by Thurston et al., demonstrating an optical instrument for pulse shaping, where the aperture was created by narrow metal strips [10].

Figure 2 displays the predicted channel shapes for a fixed bandwidth, B, of 50 GHz, while varying the OTF bandwidth, using BW_{OTF} = 8, 12, and 16 GHz. In agreement with Marom et al., a reduction in the OTF bandwidth has the effect of creating a filter shape that tends to an ideal rectangular function [9].

#141439 - $15.00 USD Received 24 Jan 2011; revised 25 Mar 2011; accepted 4 Apr 2011; published 18 Apr 2011

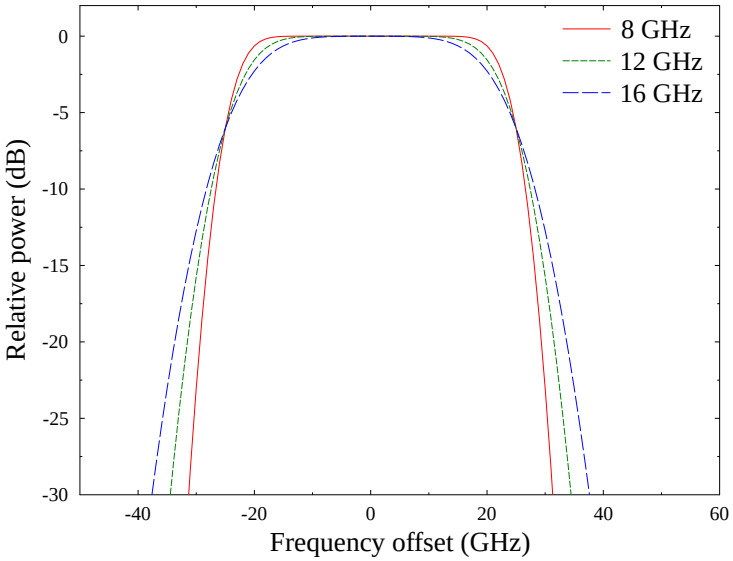

Fig. 2. The effect of the optical transfer function bandwidth on the channel shape for a 50 GHz bandpass filter response, calculated using Eq. (5) and setting B = 50 GHz and BW_{OTF} = 8, 12, and 16 GHz.

2.2. *Extension of model to a generalized WSS structure*

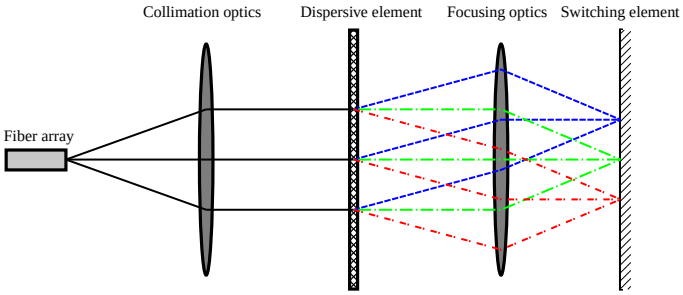

Fig. 3. Schematic of a generic WSS.

A WSS can be thought of as an optical spectrometer with a switching element in the image plane, as shown for a generic WSS in Fig. 3. Light from the input optical fiber, located in the fiber array, is collimated prior to being dispersed and imaged onto the switching element, which can be LCoS, MEMS or other technologies [11]. The switching element then directs the light into a chosen output fiber at the fiber array; note that the switching axis is perpendicular to the plane of the page, thus the output fibers are located into/out of the page. A generic WSS system was modeled in the Zemax optical design program using the physical optics propagation method [12], which allowed for examination of beam profiles at any surface and prediction of filter shapes. Figure 4a shows the spot on the switching element, and includes a Gaussian fit which indicates that the spot is highly Gaussian.

Channel shapes were predicted by creating a 50 GHz aperture at the image plane, and

#141439 - $15.00 USD Received 24 Jan 2011; revised 25 Mar 2011; accepted 4 Apr 2011; published 18 Apr 2011

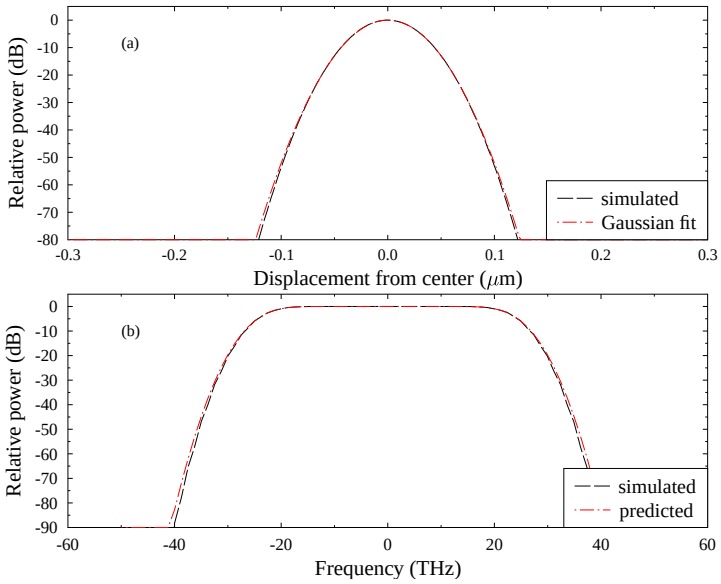

Fig. 4. Simulated WSS performance for (a) focused spot at image plane, matched to an ideal Gaussian, and (b) 50 GHz bandpass filter, matched to Eq. (5) with BW_{OTF} = 10.4 GHz and B = 50 GHz.

measuring the output coupling efficiency as a delta function in wavelength was swept through the system. As previously mentioned, the OTF bandwidth is assumed to be relatively constant over the frequency range of the WSS; one of the goals of the WSS optical design is to keep the OTF bandwidth constant over the entire spectrum. This assumption will be supported in Section 3.4, where we show measurements from a representative device.

Figure 4b shows the predicted bandshape along with a fit to Eq. (5), verifying that the generalized WSS structure produces a bandpass filter shape that matches quite well to our predicted model.

The modeling suggests that, since WSS systems use single-mode optical fiber inputs with a Gaussian profile [13], the image on the switching element will also have a Gaussian distribution. Optical aberrations in the system may cause deviations from a perfect Gaussian, but these are generally at low powers and are further suppressed by the convolution process that creates a bandshape. Note that no assumptions were made about the nature of the switching element, as the model is valid for a range of systems and switching elements.

One component that could potentially contradict our Gaussian assumption is the diffraction grating, which, in certain circumstances, produces a beam with sinc-like behaviour in the transverse field profile [14]. However, provided the diffraction grating is large enough to fit the incoming beam, then the profile of each diffraction order will match the profile of the beam incident on the grating - a Gaussian. Furthermore, the profile of each period of the diffraction grating does not affect this analysis, since it only alters the strength of each of the diffraction orders.

#141439 - $15.00 USD Received 24 Jan 2011; revised 25 Mar 2011; accepted 4 Apr 2011; published 18 Apr 2011

3. Matching filter models to spectral measurements of WSS channels

3.1. Matching supergaussian filters

The generation of a supergaussian function requires the parameters of bandwidth and supergaussian order; unlike our model, the bandwidth of a supergaussian does not represent any physical spectral width, but, rather, the width of the supergaussian spectrum at a certain level. The expression for a supergaussian function, centered at 0 Hz, is given by

$$S_{sg}(f) = \frac{1}{\sigma_{sg}\sqrt{2\pi}} \exp\left[-\left(f^2/2\sigma_{sg}^2\right)^n\right], \tag{6}$$

where n is the supergaussian order and σ_{sg} is related to the m-dB bandwidth of the supergaussian, given by

$$\sigma_{sg} = \frac{BW_{mdB}}{2\left[2\left(\ln\sqrt{10^{m/10}}\right)^{1/n}\right]^{1/2}}. \tag{7}$$

Thus, to match a supergaussian to a given WSS channel, we must first decide what power level we would like to match to, which is an undefined metric. Matching to the 20 dB level will create a spectrum that can fit the channel edges, but will not faithfully recreate the bandwidth at the top of the filter. For the purposes of this letter, we suggest matching the supergaussian to the 0.5 dB level, as it is this bandwidth that network operators are often concerned with. Setting $m = 0.5$, we must then sweep the parameter n and determine the best fit to measurement.

A disadvantage of the supergaussian approach is that this fitting routine only guarantees that the data points at the m-dB bandwidth are met, and does not match the slope of the curve.

3.2. Estimation of the optical transfer function bandwidth from measured data

The preceding analysis assumes that the optical transfer function bandwidth of the WSS is known, but in reality, devices are fabricated with a process variation that will deviate from the design target. As we have shown, the OTF bandwidth ultimately determines several of the key parameters for the final device filter shape; hence, it is of value to have a method to quickly evaluate the OTF bandwidth for each WSS module. A brute-force method could be used, i.e. sweeping the OTF bandwidth and fitting Eq. (5) to the measurement, but this can be time-consuming and problematic.

As an efficient alternative, we start by calculating the derivative with respect to frequency of Eq. (5), after it has been normalized; using properties of the error function, we find that the derivative is equal to

$$\frac{dS(f)}{df} = \frac{-1}{\sigma\sqrt{2\pi}}\left[\exp\left[-\left(\frac{B/2 - f}{\sqrt{2}\sigma}\right)^2\right] - \exp\left[-\left(\frac{-B/2 - f}{\sqrt{2}\sigma}\right)^2\right]\right]. \tag{8}$$

By inspection, we can see that the maximum/minimum values of the filter slope occur when $f = \pm B/2$, corresponding to the left- and right-hand -6.02 dB points. For example, taking $f = B/2$, we have

$$\frac{dS(f = B/2)}{df} = \frac{-1}{\sigma\sqrt{2\pi}}\left[1 - \exp\left(-B^2/2\sigma^2\right)\right]. \tag{9}$$

This reduction allows us to directly solve for the optical transfer function bandwidth as

$$BW_{\mathrm{OTF}} = 2\sqrt{2\ln 2}\exp\left[-\ln\left(-\sqrt{2\pi}\frac{dS(f = B/2)}{df}\right)\right], \tag{10}$$

#141439 - $15.00 USD Received 24 Jan 2011; revised 25 Mar 2011; accepted 4 Apr 2011; published 18 Apr 2011

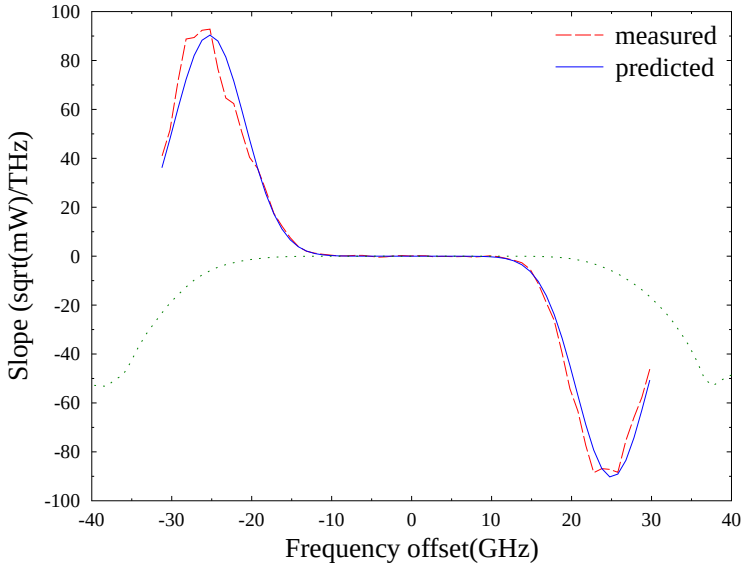

Fig. 5. The slope of a 50 GHz WSS channel, calculated numerically from a measured 50 GHz channel, and the resulting predicted slope calculated from Eq. (8). Also shown for comparison, overlaid in dotted green, is the original power spectrum measurement of the bandpass filter.

with a similar expression for the $f = -B/2$ point.

Thus, given an optical spectrum measurement of a WSS channel, the slope of the bandpass filter can be numerically evaluated, then the maximum (minimum) value used to determine the optical transfer function bandwidth. The final channel shape can then be predicted from Eq. (5), setting B to the channel width. In contrast to the supergaussian matching routine, this analysis gives the user the ability to match the edge slope; furthermore, deviations from this ideal filter response are likely to be due to misalignment or aberrations in the optical system. Thus, we can evaluate the deviation from an ideal channel shape, given a particular channel spectral measurement.

An example is shown in Fig. 5, where a measured 50 GHz channel, has been differentiated with respect to frequency. Due to measurement variation, we generally calculate two slightly different values of the OTF bandwidth based on the maximum and minimum point; both these values are compared to the measured spectrum using Eq. (10), as well as the average OTF bandwidth, allowing us to evaluate which OTF bandwidth produces the best fit to measurement. For this measured trace, we calculate the OTF bandwidth to be 10.4 GHz. The predicted slope, from Eq. (8), was generated to show the match between our model and measurement.

3.3. Comparison to measured results

To verify the accuracy of our model, we have compared measured bandpass filters generated by a Finisar WaveShaper 1000S, which uses an LCoS-based optical engine [6], but allows the creation of arbitrary bandwidth filters. The device was fed a broadband optical signal from an EDFA, then an ANDO AQ6317 optical spectrum analyzer (OSA) was used to measure the output optical power spectrum of the device under test. The OSA was set to a resolution bandwidth of 2 GHz to minimize any measurement artifacts in the power spectrum.

Figure 6 demonstrates the advantage of using this approach. A supergaussian was fitted to

#141439 - $15.00 USD Received 24 Jan 2011; revised 25 Mar 2011; accepted 4 Apr 2011; published 18 Apr 2011

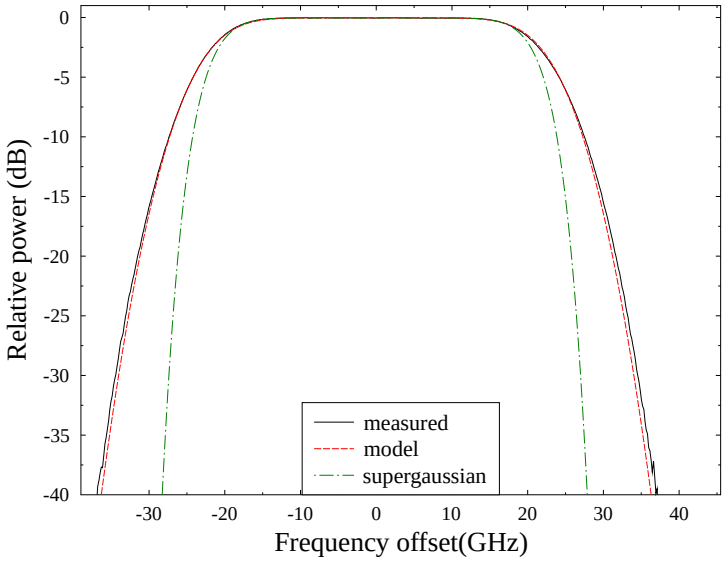

Fig. 6. A measured 50 GHz channel, compared with Eq. (5), and a supergaussian with a 0.5 dB bandwidth of 34.5 GHz and $n = 4.5$.

the 0.5 dB bandwidth of the measured data, with supergaussian order, $n = 4.5$, as detailed in Section 3.1. For the model presented in this paper, we set $B = 50$ GHz, then used the procedure outlined in Section 3.2 to determine that the OTF bandwidth, BW_{OTF}, was 10.4 GHz.

Both models replicate the 0.5 dB bandwidth accurately, but the supergaussian model deviates quickly from the channel edges; we note that a different level can be matched, for example, 6 dB or 20 dB, but this will lead to an inaccurate prediction of the 0.5 dB bandwidth, as well as changing the required supergaussian order. In contrast, the presented model requires only an evaluation of the OTF, in order to accurately construct a WSS channel.

3.4. Spectral dependence of OTF bandwidth

As discussed in Section 2.2, we have assumed that the OTF bandwidth is relatively constant over the wavelength range of the WSS; this assumption was based on the supposition that a major criteria for the optical design would be to ensure that the OTF is the same for all WSS channels. If this assumption holds for a particular WSS design, then those modules can be characterized by a single scalar value, the OTF bandwidth.

Figure 7 displays the calculated OTF bandwidth as a function of optical frequency, using the method shown in Section 3.2, for a single, representative WSS module. The mean value of the OTF bandwidth for this device is 10.7 GHz, with a standard deviation of 0.1 GHz. A linear regression was used to best-fit the data shown in Fig. 7, resulting in a line given by $BW_{\mathrm{OTF}}\,(\mathrm{GHz}) = -0.026\,f\,(\mathrm{THz}) + 15.745$ GHz. The slope of this line is deemed to be flat enough to consider the OTF bandwidth as constant over the frequency range of this device.

4. Application to next generation networks

4.1. Calculation of the m-dB bandwidth of a WSS channel

A common specification of optical filters in telecommunication networks is the 3 dB bandwidth of the filter passband. However, the design process for WSS modules may involve other band-

#141439 - $15.00 USD Received 24 Jan 2011; revised 25 Mar 2011; accepted 4 Apr 2011; published 18 Apr 2011

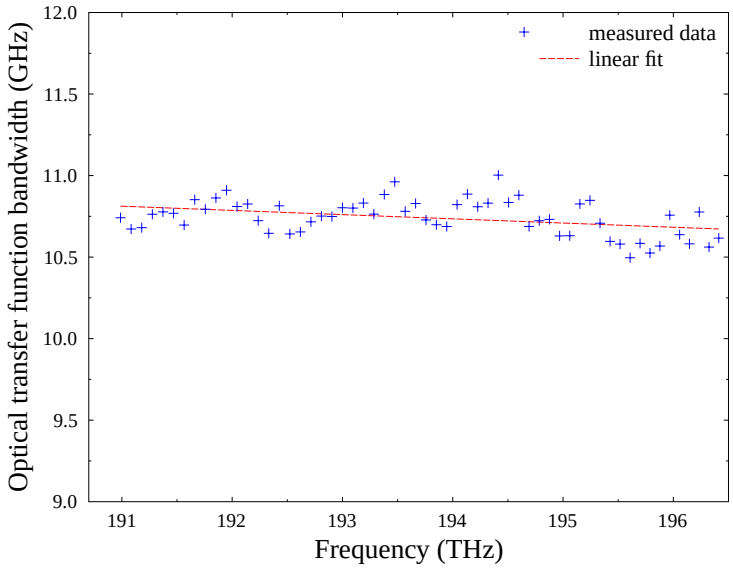

Fig. 7. Measured OTF bandwidth for a single device, evaluated over the C-band.

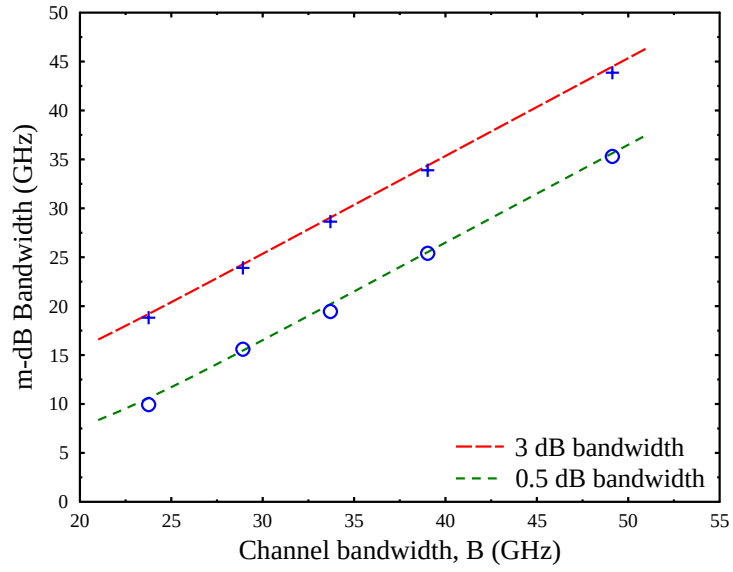

Fig. 8. Predicted 0.5 dB and 3 dB bandwidths from Eq. (12), compared to measured results (markers), for channel bandwidths ranging from 20 to 50 GHz.

#141439 - $15.00 USD Received 24 Jan 2011; revised 25 Mar 2011; accepted 4 Apr 2011; published 18 Apr 2011

width values, such as 0.5 dB or 20 dB bandwidths. Using Eq. (5), we demonstrate that the m-dB bandwidth can be predicted from this simple filter model.

We define the m-dB bandwidth as the spectral width of a filter passband at the left and right points that are m dB lower than the central peak power. That is, we are interested in the difference of the upper and lower frequencies that satisfy

$$S_{\text{m-dB}}(f) = \sqrt{10^{-m/10}} \cdot S(0). \tag{11}$$

Inserting Eq. (5) into Eq. (11), we can evaluate the m-dB bandwidth as

$$BW_{\text{m-dB}} = B - 2\sqrt{2}\sigma E_m, \tag{12}$$

where

$$E_m = \text{erfinv}\left[2\sqrt{10^{m/10}}\,\text{erf}\left(\frac{B}{2\sqrt{2}\sigma}\right) - 1\right], \tag{13}$$

where $\text{erfinv}(x)$ represents the inverse error function.

Thus, for calculation purposes, given the channel bandwidth, B we are able to match the m-dB bandwidth for a bandpass filter with arbitrary bandwidth, shown in Fig. 8. We predict the m-dB bandwidth for $m = 0.5$ dB and $m = 3$ dB, with the markers representing measurements from a previously characterized device that was found to have $\sigma = 10.0$ GHz.

It is of interest to note that the filter spectrum is exactly B GHz wide at the -6.02 dB level, which was previously identified as the location where the slope is maximum/minimum. That is, a typical 50 GHz channel in an LCoS-based WSS is 50 GHz wide at the -6.02 dB level, independent of the optical transfer function bandwidth. This is evident in Fig. 2, where the three predicted channel shapes, with different OTF bandwidth values, all intersect at the -6.02 dB level.

4.2. Prediction of cascaded WSS channels

The preceding analysis is of use in calculating the bandwidth of cascaded filters, where bandwidth narrowing is of concern in designing optical networks at bit rates of 100 Gbps or higher. Cascading WSS devices has the net effect of multiplying the bandpass filter spectra together [15], and if we assume that all the filter responses are ideal and identical, we can estimate the p-dB bandwidth of K cascaded WSS modules by:

$$BW_{\text{casc}}(p,K) = BW_{p/KdB}, \tag{14}$$

where BW_{m-dB} was given in Eq. (12). For example, the 3 dB bandwidth of 10 cascaded WSS modules can be estimated by evaluating the 0.3 dB bandwidth for a single unit.

Figure 9 shows the predicted 3 dB bandwidth of cascaded WSS filters using the model presented in this letter, compared to the supergaussian and Butterworth models. It becomes apparent that use of an inaccurate model can result in substantially different values of the overall 3 dB bandwidth of the system. Furthermore, Fig. 10 displays the resulting bandwidth narrowing from cascaded ROADMs, with the addition of showing the effect of the OTF bandwidth. Devices with a broader OTF bandwidth are predicted to be more sensitive to bandwidth narrowing, as the difference in 3 dB bandwidth between a WSS with BW_{OTF} of 8 GHz and 14 GHz grows rapidly with increasing number of cascades.

We also note that, as shown by Heismann, as well as Strasser and Wagener, manufacturing variations in center frequency and bandwidth can further cause a degradation of the system bandwidth, which may have a significant impact on the link design [4, 5]. Additionally, one major impairment in cascaded ROADMs is the accumulation of group delay ripple in the passband, but this is not considered in this paper. The analysis shown here is offered as a method to identify trends in bandwidth narrowing for cascaded ROADMs.

#141439 - $15.00 USD Received 24 Jan 2011; revised 25 Mar 2011; accepted 4 Apr 2011; published 18 Apr 2011

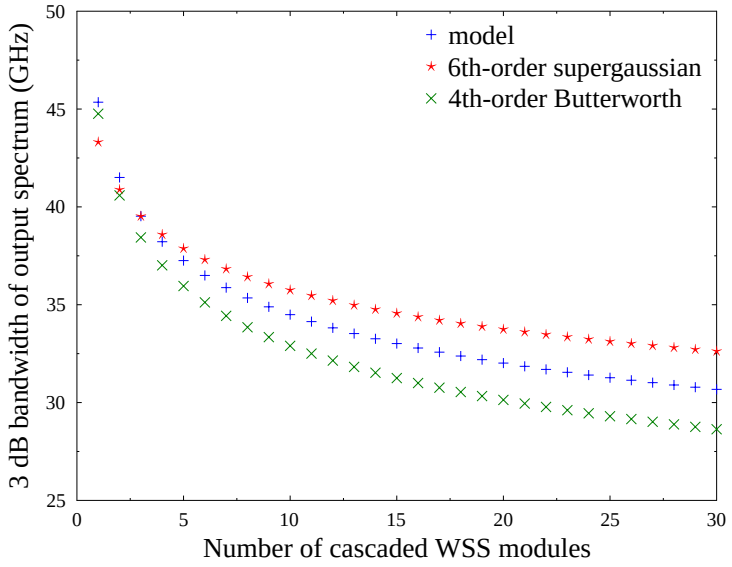

Fig. 9. Effect of cascaded WSS modules on the 3 dB bandwidth of any given channel, comparing our model to supergaussian and Butterworth filters.

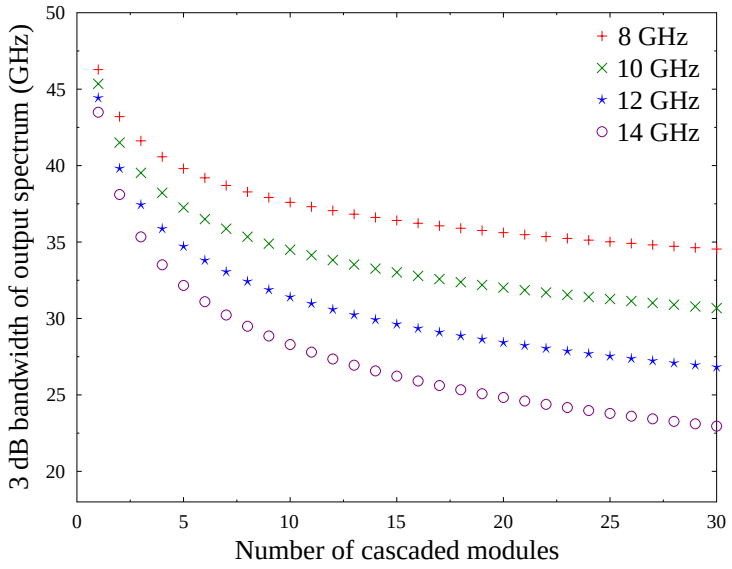

Fig. 10. Predicted 3 dB bandwidth of cascaded WSS modules, simulated for OTF bandwidths of 8, 10, 12 and 14 GHz.

#141439 - $15.00 USD Received 24 Jan 2011; revised 25 Mar 2011; accepted 4 Apr 2011; published 18 Apr 2011

4.3. *Flexible bandwidth channel plans*

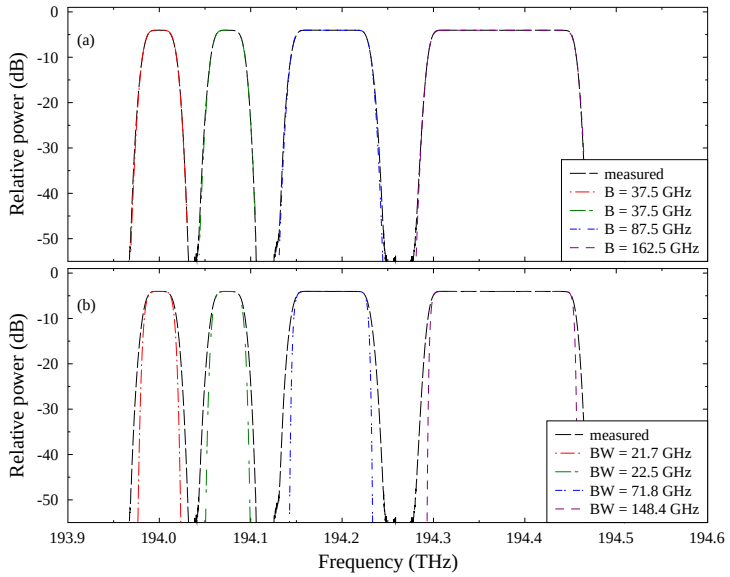

Fig. 11. Comparison between measured mixed channel plan and the matching ability of (a) the model presented in this paper, and (b) supergaussian models.

Future generations of optical networks will require WSS modules that support channels of varying bandwidth to maximize the fiber capacity. Our model is particularly suited to modeling such flexible bandwidth WSS devices. Figure 11(a) shows a comparison of our model and the supergaussian model in a mixed channel plan WSS, where we have set a spectrum with channel bandwidths of 37.5, 37.5, 87.5, and 162.5 GHz from left to right. With the model presented in this paper, we can simply match the channels shown in Fig. 11(a) with Eq. (5), using $BW_{\mathrm{OTF}} = 11.1$ GHz and B = 37.5, 37.5, 82.5, and 162.5 GHz. In this case, accurate knowledge of the optical transfer function allows a straightforward prediction of the channel shape, regardless of the channel bandwidth.

Conversely, Fig. 11(b) shows that the supergaussian model, while capable of providing a similar spectrum, requires searching through the parameter space for each channel to find the best fit. In this case, we used matching to the 0.5 dB bandwidth, where the bandwidths were used as 21.7, 22.5, 71.8, and 148.4 GHz, and the supergaussian orders were set to 3.0, 3.0, 9.8, and 22.3.

#141439 - $15.00 USD Received 24 Jan 2011; revised 25 Mar 2011; accepted 4 Apr 2011; published 18 Apr 2011

5. Conclusion

A model for predicting the spectral response of an LCoS-based WSS has been demonstrated to match experimental results better than previously published models, and uses a single characterizing parameter, the optical transfer function bandwidth, to define the optical system. The optical transfer function bandwidth is efficiently calculated by evaluating the maximum slope of a WSS bandpass filter. The increased accuracy of this approach offers a useful tool for simulation of network performance, including the cascade of WSS units in the system. Finally, we have demonstrated that this model offers a simple method of predicting channel plans involving flexible bandwidths, applicable to next- generation optical networks.

Acknowledgment

The authors would like to thank Julian Armstrong for useful discussions.

#141439 - $15.00 USD Received 24 Jan 2011; revised 25 Mar 2011; accepted 4 Apr 2011; published 18 Apr 2011